Structures and Fragmentations of Organosilicon and Organotin Radical Cations

Estelle Butcher,[a] Christopher J. Rhodes,*[,a] Mark Standing,[a] R. Stephen Davidson[b] and Richard Bowser[b]

[a] *Department of Chemistry, Queen Mary and Westfield College, University of London, Mile End Rd., London E1 4NS, UK*

[b] *Department of Chemistry, The City University, Northampton Square, London EC1V 0HB, UK*

EPR spectroscopy has been used to study radical cations derived from organosilicon and organotin compounds, as isolated in solid trichlorofluoromethane matrices at low temperatures. For the organotin radical cations depletion of electron density occurs from a unique C–Sn bond, and leads to dissociation on annealing for allyl- and benzyl-tin species, yielding allyl and benzyl radicals, respectively: remarkably, the dissociation is reversible for *p*-$MeOC_6H_4CH_2SnBu_3^{\bullet+}$ radical cations. No such fragmentation is observed for the corresponding organosilicon species, even on annealing to the melting point of the matrix (*ca.* 160 K) despite evidence that the C–Si bonds are similarly depleted on ionisation. The $Me_2N(CH_2)_3SnBu_3^{\bullet+}$ radical cation is unstable at 77 K, and fragments to form butyl radicals as the only detectable paramagnetic species.

Polymers functionalised with silicon- or tin-containing groups are of potential value as resists[1] in microlithographic processes such as the etching of microelectronic circuits. These materials may be responsive to UV, electron-beam or reactive ion-beam processing, and under such conditions ionisation to form primary molecular radical cations is to be expected. In previous photochemical studies of simple silanes and stannanes (R_4M), in the presence of molecules that are active electron acceptors when excited into their triplet states,[2] or *via* photopromoted charge transfer to various electrophiles,[3] the initially formed $R^4M^{\bullet+}$ radical cations were proposed to fragment by eqn. (1), and similarly in other systems[3–5] involving these materials which are efficient single electron donors.[6,7]

$$R_4M^{\bullet+} \longrightarrow R_3M^+ + R^\bullet \qquad (1)$$

Direct evidence for reaction (1) has been obtained for tetraalkyltin radical cations,[8,9] from which radicals R$^\bullet$ may be detected by EPR spectroscopy even under cryogenic conditions. In view of the foregoing, it seemed worthwhile to study a range of silicon- and tin-based functionalities by EPR spectroscopy in an attempt to determine any relationship between the structure and relative ease of fragmentation of their radical cations.

Results and Discussion

Results for primary radical cations as formed by γ-radiolysis of the neutral parents in solid $CFCl_3$ matrices at 77 K are displayed in Table 1. In a number of cases, secondary radicals were formed on annealing, the assignments and parameters for which are collated in Table 2.

Organotin Radical Cations

Bu_4Sn.—The spectrum recorded from tetrabutyltin at 77 K following γ-irradiation is shown in Fig. 1. There is a small yield (*ca.* 20% by double integration) of butyl radicals, which almost certainly arise from the excitation of the $Bu_4Sn^{\bullet+}$ radical cations by the exoergicity of the ($CFCl_3^{\bullet+}$/Bu_4Sn) electron transfer step, *ca.* 3.5 eV, given the difference in the ionisation potentials between $CFCl_3$ and Bu_4Sn.[10] In support of this, we observed very little further growth of these signals on annealing up to the melting point of the matrix, *ca.* 160 K, and so the $Bu_4Sn^{\bullet+}$ radical cations which are responsible for the majority of the spectrum are relatively stable once thermalised. The EPR parameters (Table 1) are very similar to those measured previously for the $Me_4Sn^{\bullet+}$ radical cation[8,9] and show that the positive hole is strongly confined to a unique C–Sn bond. Using these data with the atomic hyperfine parameters calculated by Morton and Preston[11] for the ^{119}Sn nucleus, from the Herman and Skillman wavefunction which allows for relativistic effects,[12] we obtain a negligible Sn(5s) population of 0.8% and a Sn(5p) population of 16% for the tin unit, which must therefore be planar. If the organic unit is also planar, the 14 G coupling (2 H) implies a C($2p_z$) occupancy of *ca.* 60%, but this is probably a lower limit since some bending, as was deduced for

Table 1 EPR parameters for organotin and organosilicon radical cations

Radical	Coupling constants[a]	*g* Values
$PhCH_2SnBu_3^{\bullet+}$	$A_\perp(^{117/119}Sn)$ 85; $A_\parallel$ 162	$g_\parallel$ 2.000 $g_\perp$ 2.030
$CH_2{=}CHCH_2SnBu_3^{\bullet+}$	$A_\perp(^{117/119}Sn)$ 74; *a*(2 H) 9	$g_\perp$ 2.027
H$^\bullet$–(Sn) see text	*a*(2 H) *ca.* 460	
$Bu_4Sn^{\bullet+}$	$A_\perp(^{117/119}Sn)$ *ca.* 78; $A_\parallel(^{117/119}Sn)$ *ca.* 200; *a*(2 H) 14	$g_\parallel$ 1.999 $g_\perp$ 2.047
p-$MeOC_6H_4CH_2SnBu_3^{\bullet+}$	$A_\perp(^{117/119}Sn)$ 48; $A_\parallel(^{117/119}Sn)$ 104	$g_\parallel$ 2.000 $g_\perp$ 2.020
p-$MeC_6H_4CH_2SiMe_3^{\bullet+}$	*a*(3 H) 12; *a*(2 H) 3.5; *a*(1 H) 16	*g* = 2.003
$Me_2N(CH_2)_3SiMe_3^{\bullet+}$	*a*(7 H) 28; $A_\parallel(^{14}N)$ 45	*g* = 2.003
p-$MeOC_6H_4CH_2SiMe_3^{\bullet+}$	*a*(1 H) 16; *a*(4 H) 4	*g* = 2.003
$PhCH_2SiMe_3^{\bullet+}$	*a*(1 H) 16, very poorly resolved	*g* = 2.003

[a] In G (1 G = 10^{-4} T).

Table 2 Neutral radicals formed by fragmentation of organotin and organosilicon radical cations

Radical	Coupling constants[a]	*g* Values[b]
$PhCH_2^\bullet$	*a*(2 H) 16.2; *a*(3 H) 5.6	2.0027
$CH_2{=}CH{-}CH_2^\bullet$	*a*(4 H) 14.2; *a*(1 H) 4.0	2.0026
$PhCH{=}CH{-}CH_2^\bullet$	*a*(3 H) 11.5	2.0027
$CH_3(CH_2)_2CH_2^\bullet$	*a*(3 H) *ca.* 20; *a*(1 H) 45	2.0026
p-$MeOC_6H_4CH_2^\bullet$	*a*(2 H) 15.7; *a*(2 H) 5.5	2.0028

[a] In G (1 G = 10^{-4} T). [b] Accurate to 0.0002.

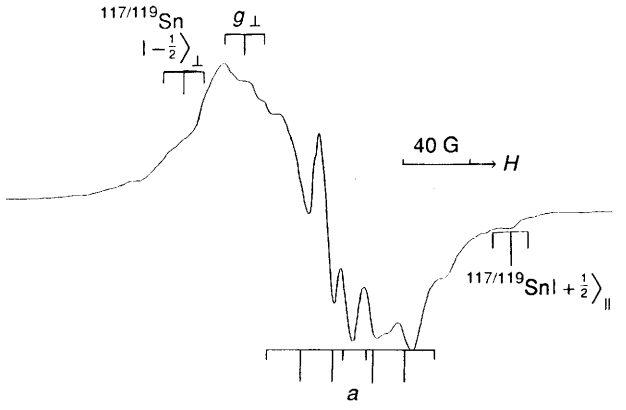

Fig. 1 EPR spectrum recorded at 77 K from Bu_4Sn following γ-radiolysis as a dilute solution in solid $CFCl_3$, and assigned to primary $Bu_4Sn^{\bullet+}$ radical cations and a smaller yield of butyl radicals (*a*)

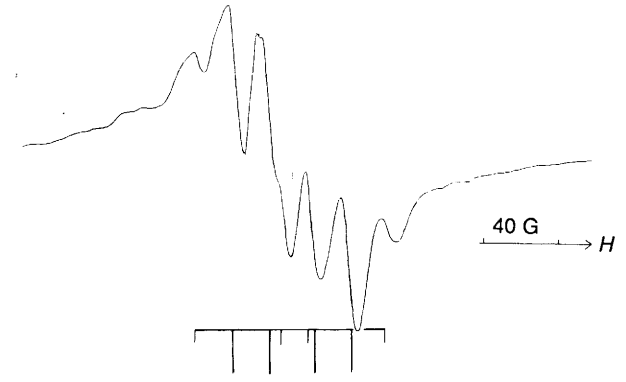

Fig. 2 EPR spectrum recorded at 77 K following γ-radiolysis of $Me_2N(CH_2)_3SnBu_3$ in a solid $CFCl_3$ matrix, showing features exclusively from butyl radicals

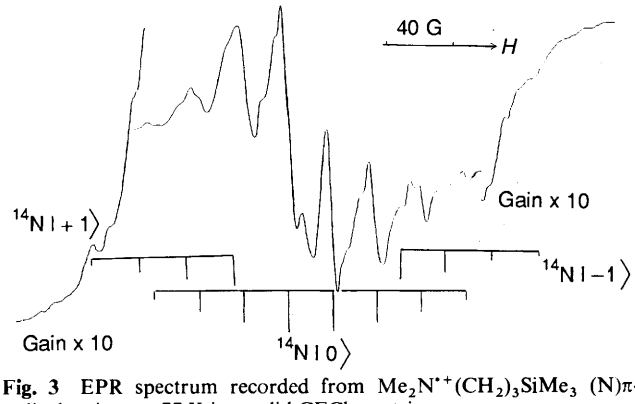

Fig. 3 EPR spectrum recorded from $Me_2N^{\bullet+}(CH_2)_3SiMe_3$ (N)π-radical cations at 77 K in a solid $CFCl_3$ matrix

the tetramethyl analogue,[8,9] will render these (negative) α couplings more positive so that they are reduced in absolute magnitude.

$Me_2N(CH_2)_3SnBu_3$ *and* $Me_2N(CH_2)_3SiMe_3$.—Fig. 2 shows an EPR spectrum recorded at 77 K from $Me_2N(CH_2)_3SnBu_3$, which can be immediately assigned to butyl radicals as the sole paramagnetic product. This is a rather interesting contrast to the behaviour of tetrabutyltin, which, under these conditions, gave a stable radical cation and only a minor yield of butyl radicals. This is particularly noteworthy because the functional change is formally remote from the metal centre, and yet the primary radical cation must be highly unstable to fragmentation, and is probably not an energy minimum (*i.e.* reorganisation of the molecular geometry following ionisation leads to the dissociation pathway). Consideration of ionisation potential data[10] for R_3N and R_4Sn compounds favours the electron loss as being from the tin unit and so the structure of the primary radical cation would be expected to be similar to that of $Bu_4Sn^{\bullet+}$. We therefore propose reaction (2) to account for the observed $C^{\bullet+}$–Sn bond cleavage.

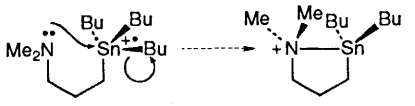

From bond energy data,[10,13] we estimate that the strength of a (virtually) one-electron C–Sn σ-bond should be *ca.* 25–20 kcal mol^{-1},* and that of a two-electron N–Sn σ-bond *ca.* 80–90 kcal mol^{-1}, so that reaction (2) will be a strongly enthalpy driven process.

Results for the silicon analogue, $Me_2N(CH_2)_3SiMe_3^{\bullet+}$, are discussed here rather than in the section on organosilicon radical cations. This species is observed (Fig. 3) as a normal nitrogen-centred π-radical[14,15] [$A_{\|}(^{14}N)$ 45 G; *a*(7 H) 27 G]. The multiplicity of the proton coupling is at first sight curious, but must mean that the CH_2X group [X = $(CH_2)_2SiMe_3$] is oriented as in **1** so that one C–H_A bond subtends a dihedral

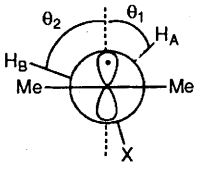

1

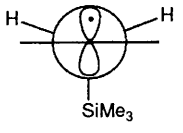

5

angle (θ_1) with respect to the N(2p) orbital of *ca.* 45°, giving a coupling equal to that for a freely rotating methyl group, while the other C–H_B lies close to the nodal plane (**1** predicts θ_2 = 75°; *a* < 4 G, unresolved). This result is in agreement with ionisation potential data for R_3N and R_4Si compounds,[10] and with previous mechanistic conjecture from photochemical studies of compounds of this type.[16]

$PhCH_2SnBu_3$ *and* p-MeO-$C_6H_4CH_2SnBu_3$.—Fig. 4(*a*) shows the spectrum recorded at 77 K, following radiolysis of $PhCH_2SnBu_3$ in solid $CFCl_3$. There is an intense feature from the perpendicular component of non-magnetic tin complexes which defines $g_{\perp}$ = 2.030 and, associated with this, is the $|-\frac{1}{2}\rangle$ $A_{\perp}(^{117/119}Sn)$ feature, yielding the value $A_{\perp}(^{117/119}Sn)$ = 85 G. The $g_{\|}$ feature is less readily located within the central region because of the presence of butyl radicals, but is most likely the peak at 2.000. In the high field region of the spectrum are two parallel peaks (α,β) which are possible contenders for the $|+\frac{1}{2}\rangle$ $^{117/119}Sn$ transition. From α a value of $A_{\|}(^{117/119}Sn)$ = 162 G is obtained, leading to a Sn(5p) population of 0.10; on the other hand, values of $A_{\|}(^{117/119}Sn)$ = 190 G and Sn(5p) population = 0.13 are derived from the field position of β. Given that the shift of the *g*-component from free-spin is determined largely by the occupancy of the 5p level, it may be anticipated that the ratios of the *g*-shifts and 2*B* values for two structurally related $R_4Sn^{\bullet+}$ radicals should be roughly the same. The $g_{\perp}$ value (Table 1) in the $Bu_4Sn^{\bullet+}$ radical cation is 2.047, so that $\Delta g(PhCH_2SnBu_3^{\bullet+})/\Delta g(Bu_4Sn^{\bullet+})$ = 0.64; the corresponding ratio of 2*B* values is either 0.63(α) or 0.81(β), and so we favour α as the correct parallel feature, giving the parameters in Table 1. Since there is no resolved proton coupling, we are unable to estimate the spin distribution in the remainder of this

* 1 cal = 4.184 J.

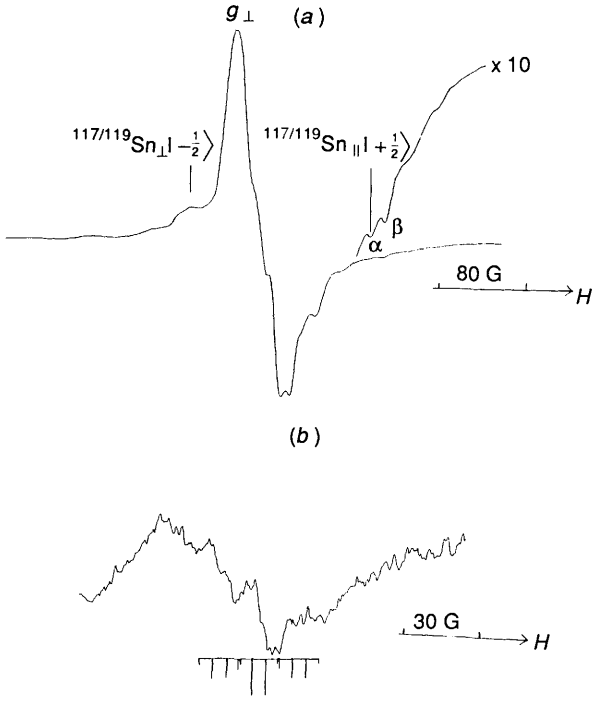

Fig. 4 EPR spectra recorded from $PhCH_2SnBu_3^{\bullet+}$ radical cations in a $CFCl_3$ matrix, (*a*) at 77 K, (*b*) at 155 K, showing weak features from free benzyl radicals

system, but consider that the reduction in $g_\perp$ and in $2B$ from those in the tetraalkyl analogues reflects some delocalisation of the positive hole from the electron-depleted (benzyl)C–Sn bond onto the aromatic group. On annealing to *ca.* 155 K, an overall loss of the signal occurred, but a new set of features appeared [Fig. 4(*b*)] with a(2 H) = 16.2 G, a(3 H) = 5.6 G and g = 2.0027, which can readily be assigned to free benzyl radicals. This accords with our structural view of an electron depleted C–Sn bond which fragments *via* eqn. (3), as was the case for dibenzylmercury radical cations.

$$PhCH_2^{\bullet+}\text{–}SnBu_3 \longrightarrow PhCH_2^{\bullet} + {}^{+}SnBu_3 \qquad (3)$$

The *p*-methoxy analogue possesses markedly reduced $g_\perp$ and $A_\perp$ components (Table 1), and thus the Sn(5p) population is considerably less than in the unsubstituted case. Again, there is some ambiguity regarding the assignment of the parallel $|+\frac{1}{2}\rangle$ feature, but that shown [Fig. 5(*a*)] agrees with the $g_\perp$ shift [*i.e.* the ratios of $g_\perp$ and of $2B$ are (0.40, 0.46) and (0.60, 0.64) with $Bu_4Sn^{\bullet+}$ and $PhCH_2SnBu_3^{\bullet+}$ respectively]. On annealing to 140 K, features assigned to p-$MeOC_6H_4CH_2^{\bullet}$ radical grew-in with concommitant reduction of those from intact primary radical cations [Fig. 5(*b*)]. However, this was found to be a reversible process, since recooling to 77 K [Fig. 5(*c*)] resulted in the regeneration of the original radical cation signal with minimal loss in intensity. This behaviour was not observed with $PhCH_2SnBu_3^{\bullet+}$ radical cations, which may be simply because it was necessary to anneal to the matrix softening temperature (155 K) in order to observe the fragmentation (3), at which point the radicals diffuse and are destroyed by combination reactions. The requirement of a lower temperature in the latter case shows that the C–Sn bond is weakened by the *p*-methoxy substitution, or more precisely that the activation energy for the dissociation is reduced. This is quite surprising, since considerations based on bond energy[10,13] and ionisation potential[10] data predict that the reverse would probably be the case, and that the alternative spin/charge separation to reaction (3) should occur leading to the less electron affinic p-$MeOC_6H_4CH_2^{+}$ cation,

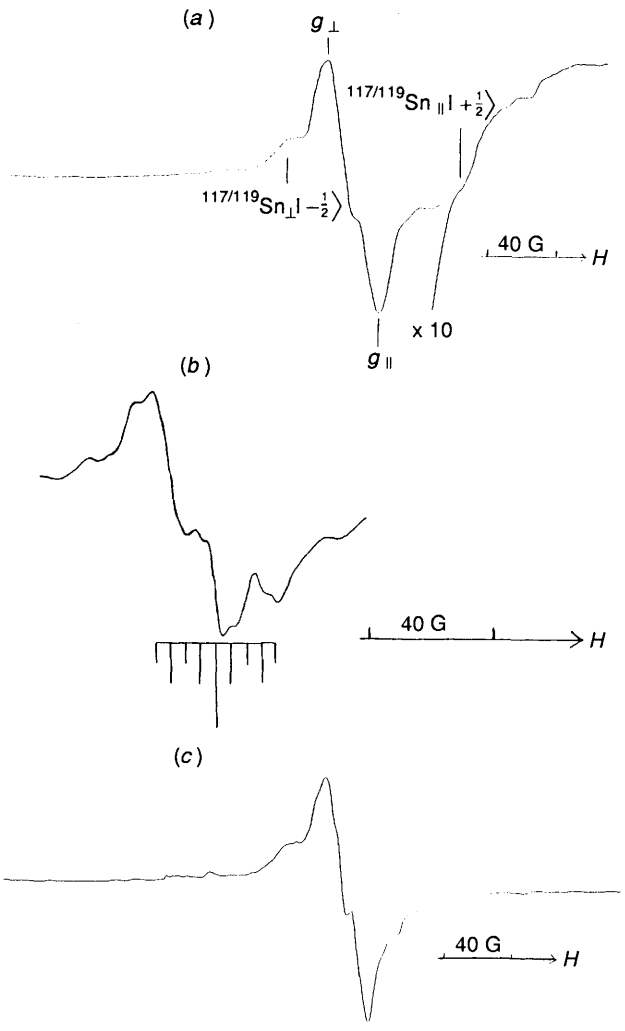

Fig. 5 EPR spectra recorded from p-$MeOC_6H_4CH_2SnBu_3^{\bullet+}$ radical cations, (*a*) at 77 K, (*b*) at 140 K, showing features from p-$MeOC_6H_4CH_2^{\bullet}$ free radicals, (*c*) after re-cooling to 77 K, showing regeneration of primary radical cations (see text)

which has a lower electron affinity, along with the $Bu_3Sn^{\bullet}$ radical. Additionally, the Sn(5s,5p) orbital populations show that the C–Sn bond is less depleted of electron density in the *p*-MeO case and is therefore stronger in the ground state, because this substituent is more able to localise the positive hole to the aromatic ring. We therefore propose Scheme 1 in

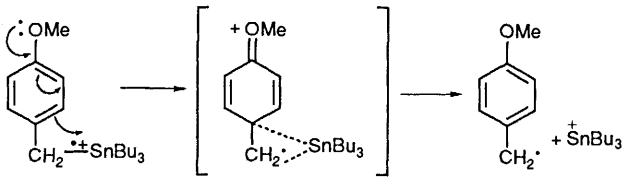

Scheme 1

which the cleavage of the $C^{\bullet+}$–Sn bond is assisted by the greater electron releasing power of the ring; this mechanism would also account for the observed direction of the bond cleavage.

The proton hyperfine couplings in the resulting *p*-methoxybenzyl radical are not significantly perturbed from those measured in fluid solution,[17] and so any subsequent π-interaction between this and the Bu_3Sn^{+} cation can only be weak. However, these fragments do not separate completely because the $CFCl_3$ matrix is still rigid at 140 K and prevents this; on cooling again to 77 K, the radical/cation pair recombine

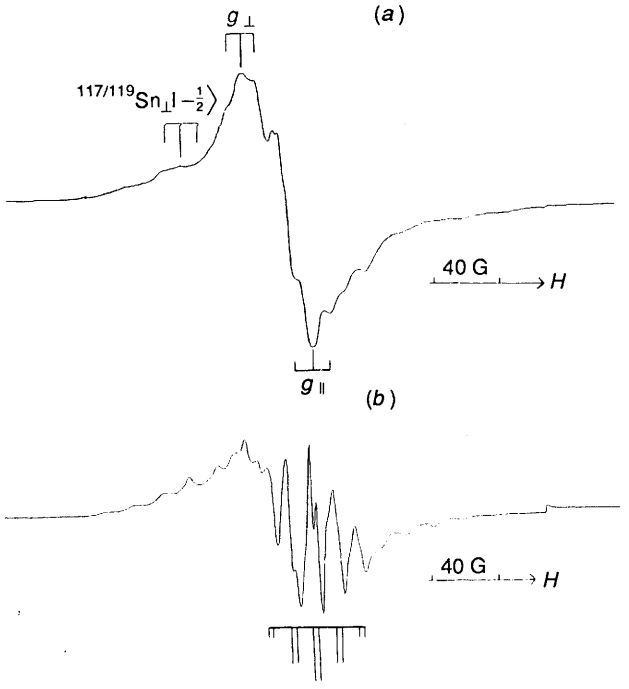

Fig. 6 EPR spectra recorded (*a*) from CH_2=$CHCH_2SnBu_3^{\bullet+}$ radical cations at 77 K, (*b*) from sample in (*a*) at 120 K, showing features from free allyl radicals

Table 3 Spin populations and estimated configurations for tin-centred radical cations

Radical	5s	5p	p + s	p/s	θ/°
$Me_4Sn^{\bullet+}$ [a,b]	0.008	0.168	0.178	21	118
$Bu_4Sn^{\bullet+}$	0.008	0.156	0.164	21	118
$PhCH_2SnBu_3^{\bullet+}$	0.007	0.098	0.105	14	117
p-$MeOC_6H_4CH_2SnBu_3^{\bullet+}$	0.004	0.071	0.075	16	117
CH_2=$CHCH_2SnBu_3^{\bullet+}$	0.006[c]	0.086[d]	0.093	13	116

[a] Ref. 8. [b] Ref. 9. [c] Obtained from eqn. (4). [d] Estimated from $g_\perp$ shift.

to form the original structure. We note that a similar reversible dissociation of the $Bu^tSnMe_3^{\bullet+}$ ($\rightleftharpoons Bu^{t\bullet} + {}^+SnMe_3$) radical cation was reported by Symons and co-workers.[9]

H_2C=$CHCH_2SnBu_3$ *and* PhCH=$CHCH_2Bu_3$.—The spectrum recorded from the allyl derivative is shown in Fig. 6(*a*) and again comprises an intense perpendicular *g* feature (2.027) and its associated $|-\frac{1}{2}\rangle$ ($^{117/119}Sn$) component. Unfortunately, the $|+\frac{1}{2}\rangle_\parallel$ ($^{117/119}Sn$) feature is not readily discernible among signals from other radicals formed in small yield. Therefore, we are unable to evaluate the tin orbital populations as we have in the previous examples. However, comparison of the perpendicular *g*-shift from free-spin with those of the other radicals, whose hyperfine tensors are fully determined, allows an estimate of the 5p orbital population at 8.6%, and the 5s spin population can then be determined from eqn. (4), where B_0 and A_0 are taken

$$\rho 5s = (A_\perp + \rho 5p \cdot B_0)/A_0 \quad (4)$$

from Morton and Preston's data.[11] The 5p/5s ratio is 13 and it may be taken that the tin centre is marginally more pyramidal in this case than in the others (Table 3), although this may be partly an artefact caused by the different procedure used.

There is also some further structure present on the central features, which we assign to a *ca.* 9 G coupling to the two equivalent protons on the terminal carbon atom, and so the spin

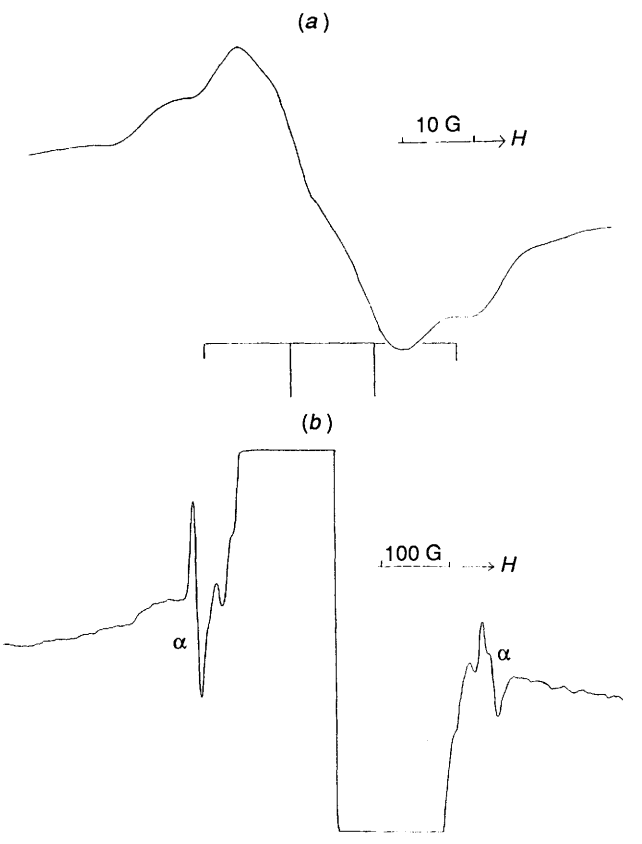

Fig. 7 EPR spectra recorded from PhCH=$CHCH_2SnBu_3$ following γ-radiolysis in solid $CFCl_3$ at 77 K, (*a*) showing features assigned to PhCH=$CHCH_2^{\bullet}$ radicals, (*b*) at higher gain and wider expansion, showing features (α) from H-atom/Sn complex (see text)

density at this position is *ca.* 40%. By a relatively modest increase in the temperature (to 120 K), features immediately recognisable as belonging to free allyl radicals[18] were observed [Fig. 6(*b*)], concomitantly with the loss of the initial $g_\perp$ feature from the primary radical cations. This shows that the activation energy for C–Sn bond cleavage [eqn. (5)] is reduced from those for the benzyl analogues, and it is noteworthy that the process is not reversible, despite the fact that the $CFCl_3$ matrix is still rigid over the temperature range (77–140 K) used in this experiment. A simple explanation for the former result is a product development argument based around the greater stability of an allyl than a benzyl radical.[10] The non-reversible nature of reaction (5) may relate to higher C···C bond orders, because of the higher symmetry of the allyl radical, which leads to a greater resistance to bending of the carbon centre in the developing C···Sn bond than is the case for a benzyl radical. We stress that this is a speculative view, but note that differences in 'reorganisation energies' of carbon centres (pyramidal to planar) have been invoked previously[19,20] to account for changes in the relative ease of bond homolyses (*i.e.* the reverse of the present situation), in terms of the changes in geometry that must accompany them (C–X ⟶ $C^\bullet$ + $X^\bullet$). Fig. 6(*b*) also seems to show an increased yield of $CFCl_2^\bullet$ radicals, and it may be that the alternative reaction (6) also occurs leading to tin-centred radicals that abstract chlorine atoms from the matrix [eqn. (7)].

$$CH_2{=}CHCH_2SnBu_3^{\bullet+} \longrightarrow CH_2{=}CHCH_2^\bullet + {}^+SnBu_3 \quad (5)$$

$$CH_2{=}CHCH_2SnBu_3^{\bullet+} \longrightarrow CH_2{=}CHCH_2^+ + {}^\bullet SnBu_3 \quad (6)$$

$$Bu_3Sn^\bullet + CFCl_3 \longrightarrow Bu_3SnCl + CFCl_2^\bullet \quad (7)$$

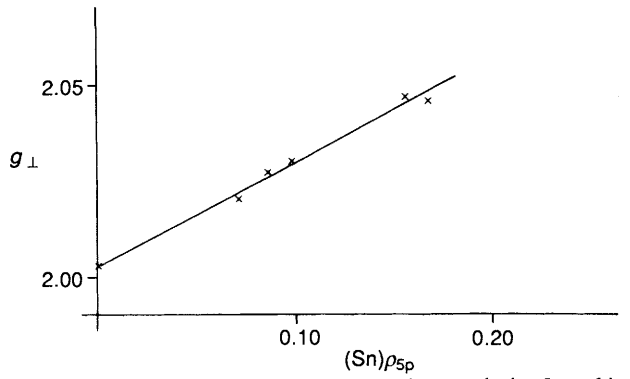

Fig. 8 Linear correlation between $g_\perp$ values and tin 5p orbital populations for organotin radical cations

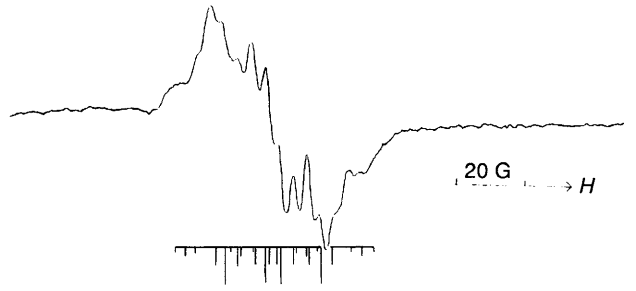

Fig. 9 EPR spectrum recorded from *p*-$MeC_6H_4CH_2SiMe_3^{\bullet+}$ radical cations at 77 K in a solid $CFCl_3$ matrix

Fig. 7(*a*) shows the spectrum recorded following γ-irradiation of $PhCH{=}CHCH_2SnBu_3$ in solid $CFCl_3$ at 77 K, and is seen to comprise a pattern of four broad lines with a common separation of *ca.* 11.5 G, along with some weaker signals. We feel that these are best assigned to $PhCH{=}CHCH_2^\bullet$ radicals, in which case the primary radical cations are already unstable at 77 K. Most interestingly, the wing regions of the spectrum [Fig. 7(*b*)] show features with the relatively large separation of *ca.* 460 G. The low field line appears to be isotropic, but the high field line shows an apparent ||,⊥ splitting consistent with *g*/*A* anisotropy. We suggest that this centre is a tin/H-atom adduct, and arises from the dissociation (8) followed by a reassociation

$$PhCH{=}CHCH_2SnBu_3^{7\bullet+} \longrightarrow PhCH{=}\overset{+}{C}HCHSnBu_3 + H^\bullet \quad (8)$$

between the H-atom and the tin unit. We considered the possibility that these are just the extreme features of a more complex pattern which is largely concealed by the intense central lines, but a chemical structure that would accommodate an interpretation along these lines is far less obvious. Since the H(1s) population is *ca.* 91%, we require a bonding scheme involving a vacant, relatively high energy, orbital on tin so that the H–Sn bonding depletes the H(1s) orbital to only a relatively small extent [*i.e.* the bonding orbital is still mainly H(1s)]. This could be accomplished (**2**) using the tin ($5d_{z^2}$) orbital, but since

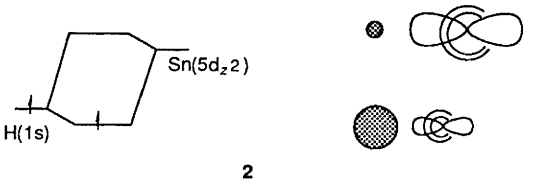

2

the spectrum does not provide unambiguous evidence for the $^{117/119}Sn$ satellite features, we are unable to comment further.

Correlation between $g_\perp$ *and* Sn(5p) *Orbital Populations.*—In our previous study of diphenyl- and dibenzyl-mercury radical cations,[21] we obtained a good linear correlation between $g_\perp$ and $A_\perp(^{199}Hg)$, because the *g*-shift from free-spin is determined mainly by the spin population in the Hg(6p) atomic orbital and the C–Hg–C unit possesses essentially the same (linear) structure and 6p/6s ratio throughout the series. In the present case, a rather poor correlation was obtained, because there is variation in the configuration of the tin centres (Table 3), becoming more planar as the depletion of electron density from the $C^{\bullet+}$–Sn bond increases. Therefore it is necessary to plot $g_\perp$ against the Sn(5p) population directly, in which case a good correlation is obtained (Fig. 8), as expected *if it is this* quantity alone that dominates the shift of $g_\perp$ from free-spin. Any changes in $g_\parallel$ were only very minor and are not considered to be structurally diagnostic. However, the fact that these (g_{zz}) values are all reduced from free-spin shows that the unpaired electron is not in a pure 5s/5p hybrid orbital, but that a non-axial component permits mixing with higher (vacant) orbitals along the *z*-axis.

Organosilicon Radical Cations

p-$MeC_6H_4CH_2SiMe_3$, $PhCH_2SiMe_3$ *and* p-$MeOC_6H_4CH_2SiMe_3$.—In Fig. 9 is shown the spectrum obtained from *p*-$MeC_6H_4CH_2SiMe_3^{\bullet+}$ radical cations. This may be reconstructed by a pattern of couplings from: *a*(3 H) 12 G, *a*(1 H) 16 G, *a*(3 H) 3.5 G. We therefore propose that the SOMO is the ψ_s (b_1) orbital (**3**) and assumption of approximately equal spin

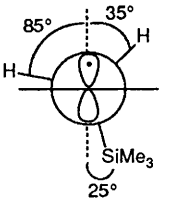

4

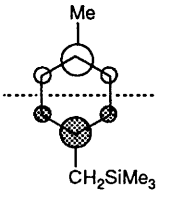

3

populations of the $C(2p_z)$ atomic orbitals at the 1,4 positions along with the usual $B\cos^2\theta$ dependence of the β–C–H coupling indicates that the CH_2–$SiMe_3$ group is oriented as in **4**; the coupling to the other β-C–H proton is predicted to be only 0.2 G and is not therefore resolved. Therefore, although the silyl group adopts a position for effective hyperconjugation, it is not fully aligned with the adjacent ring atomic p orbital. One could argue that this conformation compromises hyperconjugative overlap with *both* C–H and C–Si bonds, but previous results for alkyl radicals such as $Me_3SiCH_2CH_2^\bullet$[22,23] show that it is the β-silyl group that dominates, and the effect is enhanced in cationic species.[24] Results obtained by Bock and Kaim[25] for a range of aromatic radical cations with Me_3SiCH_2 substituents, measured in fluid solution, show that in general the fully eclipsed conformation (**5**) is preferred. However, the coupling measured in the liquid state is averaged over the torsional states of the C–C(Si) bond and does not give precise details of the minimum energy conformation as measured in the solid state, which may in any case be influenced by matrix effects. Liquid phase results for the *p*-bis(trimethylsilylmethyl)benzene radical cation[25] show that the ψ_s (b_1) orbital is the SOMO and that all four CH_2(–$SiMe_3$) protons are equivalent under the conditions of measurement [*a*(4 H) = 8.4 G]; the silylmethyl substituents apparently delocalise spin density from the system to the extent of only *ca.* 2%. In the less symmetrical *p*-$MeC_6H_4CH_2SiMe_3^{\bullet+}$ radical cation, it is clear that the single Me_3SiCH_2 substituent exerts a profound influence on the unpaired electron distribution most noticeably because the coupling to the *p*-Me protons is reduced to 60% of that measured for the $MePh^{\bullet+}$ radical cation.[26]

A strong bonding interaction between the b_1 and σ_{C-Si} orbitals will lead to a resulting $\psi(b_1)$–$\psi(\sigma)$ combination in which the spin density on the unsubstituted ring positions is greater at the *ortho* than at the *meta* carbon atoms, but with

substantial density in the σ_{C-Si} region[27,28] (*i.e.* approaching that expected for a 'benzylic' PhX$^{\bullet}$ SOMO). We thus assign the (2 H) 3.5 G coupling to the *ortho* protons[29] and estimate that the total spin density on the ring is *ca.* 70% and *ca.* 30% in the C–Si bond. Spin density on the benzylic carbon atom might be expected to contribute to the coupling of the attached (α) protons, but as with the benzyltin analogues, the overall effect of this may be virtually zero for a pyramidal configuration in which the direct (positive) and spin-polarisation (negative) contributions cancel.

The spectra of the other benzylsilane radical cations are less conclusive owing to their poor resolution. This was improved somewhat following annealing to 150 K, when both then appeared to show dominantly a *ca.* 16 G doublet splitting, and thus conformations similar to **5** may pertain in these cases also. For none of these organosilane radical cations could we detect definitively the formation of free benzyl radicals, even on annealing up to the melting point of the matrix, *ca.* 160 K.

Structure and Stability

Specific cases have already been discussed, but we conclude with some general points. There is a definite depletion of electron density from the C–Sn(Si) bonds on ionisation in all the compounds studied. Since the benzylic and allylic C–Sn bonds are intrinsically weak (*ca.* 40 kcal mol^{-1}) it is these that cleave most readily in the radical cations. We observe that the ease of fragmentation [eqn. (1)] in these species does not, however, follow the order of electron depletion, but instead appears to relate to the stabilisation of the developing radical/cation fragments [*i.e.* a transition-state effect]. Fragmentations of benzylsilane radical cations were not observed under our conditions and so the point is made that C$^{\bullet+}$–Si bond cleavages occur less readily than C$^{\bullet+}$–Sn bond cleavages. Thus it is the benzyltin compounds that are anticipated to be the more responsive to the influence of radiation under ionising conditions and thus act as better resist functionalities.

Experimental

The details of the preparation of the silicon and tin compounds will be reported elsewhere.[30] Tetrabutyltin was purchased from Aldrich and purified by fractional distillation. Trichlorofluoromethane was purchased from BDH and Fluka and was purified by filtration through activated silica immediately prior to use in order to reduce matrix signals formed by γ-irradiation. Dilute (0.1–1.0 wt%) solutions of the organometallic substrates were prepared in the freon solvent, and were frozen to 77 K in liquid nitrogen to form polycrystalline solids, which were subsequently irradiated to a dose of 1 Mrad using a ^{60}Co source. EPR spectra were recorded using either Bruker ER 200D or Varian E9 spectrometers, normally at 77 K, and samples were annealed above this temperature initially by simply decanting the nitrogen coolant from the insert Dewar and allowing the sample to warm, while continuously monitoring the EPR signal for changes, or using a standard Bruker or Varian variable temperature device when specific temperatures were required.

Acknowledgements

We thank the SERC and the following companies for support of CASE awards: Courtaulds Coatings (to E. B.), Ceram Research (to M. S.), and Dr. P. G. Clay for providing access to facilities for ^{60}Co γ-irradiation.

References

1 *The Effects of Radiation on High-Technology Polymers*, eds. E. Reichmann and J. H. O'Donnel, American Chemical Society, Washington DC, 1989.
2 S. Kyushin, Y. Masuda, K. Matsushita, Y. Nakadaira and M. Ohashi, *Tetrahedron Lett.*, 1990, 6395.
3 J. K. Kochi, *Organometallic Mechanisms and Catalysis*, Academic Press, New York, 1978, Part III.
4 C. L. Wong and J. K. Kochi, *J. Am. Chem. Soc.*, 1979, **101**, 5593.
5 R. J. Klingler and J. K. Kochi, *J. Am. Chem. Soc.*, 1980, **102**, 4760.
6 R. Boschi, M. F. Lappert, J. B. Pedley, W. Schmidt and B. T. Wilkins, *J. Organomet. Chem.*, 1973, **50**, 69.
7 S. Evans, J. C. Green, P. J. Joachim, A. F. Orchard, D. W. Turner and J. P. Maier, *J. Chem. Soc., Faraday Trans. 2*, 1979, **68**, 905.
8 B. W. Walther, F. Williams, W. Lau and J. K. Kochi, *Organometallics*, 1983, **2**, 688.
9 A. Hasegawa, S. Kaminaka, T. Wakabayashi, M. Hayashi, M. C. R. Symons and J. Rideout, *J. Chem. Soc., Dalton Trans.*, 1984, 1667.
10 V. I. Vedeneyev, L. V. Gurvich, V. N. Kondrat'yev, V. A. Medvedev and Ye. L. Frankevich, *Bond Energies, Ionisation Potentials and Electron Affinities*, Arnold, London, 1966.
11 J. R. Morton and K. F. Preston, *J. Magn. Reson.*, 1978, **30**, 577.
12 F. Herman and S. Skillman, *Atomic Structure Calculations*, Prentice-Hall, Englewood Cliffs, N.J., 1963.
13 J. E. Huheey, *Inorganic Chemistry. Principles of Structure and Reactivity*, Harper and Row, New York, 1978.
14 C. J. Rhodes, *J. Chem. Soc., Perkin Trans. 2*, 1992, 235.
15 G. W. Eastland, D. N. R. Rao and M. C. R. Symons, *J. Chem. Soc., Perkin Trans. 2*, 1984, 1551.
16 E. Hasegawa, W. Xu, P. S. Mariano, U.-C. Yoon and K.-U. Kim, *J. Am. Chem. Soc.*, 1988, **110**, 8099.
17 J. M. Dust and D. R. Arnold, *J. Am. Chem. Soc.*, 1983, **105**, 1221; 6531.
18 J. K. Kochi and P. J. Krusic, *J. Am. Chem. Soc.*, 1968, **90**, 7157.
19 C. J. Rhodes and M. C. R. Symons, *J. Chem. Soc., Faraday Trans. 1*, 1987, 258.
20 T. N. Bell and P. G. Perkins, *J. Phys. Chem.*, 1977, **81**, 2012.
21 C. J. Rhodes, C. Glidewell and H. Agirbas, *J. Chem. Soc., Faraday Trans.*, 1991, 3171.
22 P. J. Krusic and J. K. Kochi, *J. Am. Chem. Soc.*, 1971, **93**, 846.
23 A. R. Lyons and M. C. R. Symons, *J. Chem. Soc., Faraday Trans. 2*, 1972, **68**, 622.
24 W. Hanstein, H. J. Berwin and T. G. Traylor, *J. Am. Chem. Soc.*, 1970, **92**, 829.
25 H. Bock and W. Kaim, *Chem. Ber.*, 1978, **111**, 3552.
26 D. N. R. Rao and M. C. R. Symons, *J. Chem. Soc., Perkin Trans. 2*, 1985, 991.
27 V. F. Traven, M. Yu. Eismont, V. V. Redchenko and B. I. Stepanov, *Zh. Obsch. Khim.*, 1980, **50**, 2001.
28 V. F. Traven, V. V. Redchenko and B. I. Stepanov, *Zh. Obsch. Khim.*, 1982, **52**, 2262.
29 C. J. Rhodes, *J. Organomet. Chem.*, 1988, **356**, 17.
30 R. S. Davidson and R. Bowser, to be published.

Paper 2/01830F
Received 30*th March* 1992
Accepted 27*th May* 1992